V_2O_5/TiO_2 Catalytic Xerogels Raman and EPR Studies

CRISTIANE B. RODELLA, ROBERTO W.A. FRANCO, CLAUDIO J. MAGON, JOSE P. DONOSO AND LUIS A.O. NUNES
Instituto de Física, USP-São Carlos, C.P. 369, CEP: 13560-970, São Carlos, SP, Brazil

MARGARIDA J. SAEKI
Departamento de Química, FC, UNESP, C.P. 473, CEP: 17033-360, Bauru, SP, Brazil

MICHEL A. AEGERTER
Institut für Neue Materialien, 66123 Saarbrücken, Germany

VAGNER SARGENTELLI AND ARIOVALDO O. FLORENTINO*
Departamento de Química e Bioquímica, IB, UNESP, C.P. 510, CEP: 18618-000, Botucatu, SP, Brazil
arif@ibb.unesp.br

Received December 8, 2000; Accepted March 6, 2002

Abstract. Raman spectroscopy and Electron Paramagnetic Resonance (EPR) studies were performed on a series of V_2O_5/TiO_2 catalysts prepared by a modified sol-gel method in order to identify the vanadium species. Two species of surface vanadium were identified by Raman measurements, monomeric vanadyls and polymeric vanadates. Monomeric vanadyls are characterized by a narrow Raman band at 1030 cm^{-1} and polymeric vanadates by two broad bands in the region from 900 to 960 cm^{-1} and 770 to 850 cm^{-1}. The Raman spectra do not exhibit characteristic peaks of crystalline V_2O_5. These results are in agreement with those of X-ray Diffractometry (XRD) and Fourier Transform Infrared (FT-IR) previously reported (C.B. Rodella et al., J. Sol-Gel Sci. Techn., submitted). At least three families of V^{4+} ions were identified by EPR investigations. The analysis of the EPR spectra suggests that isolated V^{4+} ions are located in sites with octahedral symmetry substituting for Ti^{4+} ions in the rutile structure. Magnetically interacting V^{4+} ions are also present as pairs or clusters giving rise to a broad and structureless EPR line. At higher concentration of V_2O_5, a partial oxidation of V^{4+} to V^{5+} is apparent from the EPR results.

Keywords: catalyst, vanadium and titanium oxides, sol-gel, characterization

Introduction

Vanadium-titanium oxides constitute a well-known catalytic system for selective oxidation reactions [1–3]. The outstanding catalytic behavior of vanadia supported on titania in comparison to other oxides such as SiO_2 or Al_2O_3, is attributed to the strong support-active phase interaction. It has been shown that a higher activity and selectivity is achieved when vanadia is supported on anatase rather than on rutile.

The major disadvantage of the titania support prepared by conventional ceramic processes is its low specific surface area. In addition, the anatase phase has a poor thermal stability at high temperature. Its partial transformation into rutile is thermodynamically favored but leads to a worsening of catalytic performance.

*To whom all correspondence should be addressed.

As the characteristics of the support are fundamental for the stabilization of the active phase in V_2O_5/TiO_2 catalysts and depend mainly on the preparation methods, several efforts are being made to develop new oxide supports to satisfy the needs of practical application [1–4].

A new route using a modified sol-gel method was proposed for the preparation of V_2O_5/TiO_2 catalysts [5]. The samples show an increase of the (BET) surface area with the increased loading, and an absence of crystalline V_2O_5. This system shows a high activity for ethanol oxidation [5].

Vibrational spectroscopy has been used to characterize the structure of highly dispersed VO_x species present on the surface of TiO_2 [6]. For low concentrations of V_2O_5, monomeric vanadyls are the primary species present on TiO_2 supports. This species is characterized by a narrow peak near 1030 cm^{-1} in both the Fourier Transform Infrared (FT-IR) and Raman spectra, indicative of a very strong V=O bond. As the vanadia loading increases, new Raman bands appear in the region of 800–1000 cm^{-1}, attributed to the terminal V=O bonds of polymeric vanadia species [6].

Electron Paramagnetic Resonance (EPR) also has been successfully applied to the study of V_2O_5/TiO_2 catalysts [1–3, 7–10]. The technique is a powerful tool for determining the coordination environment of paramagnetic centers, such as transition metal ions. The V^{4+} ion is a particularly useful probe since its EPR spectrum is readily observable over a large temperature range. Spin Hamiltonian parameters obtained from such spectra are very sensitive to the nature of the support (anatase or rutile), the location (surface, interstitial or substitutional) and the symmetry of the site of the ion in the TiO_2 matrix [9, 11].

The present paper reports additional investigation carried out with Raman and EPR spectroscopy on a series of V_2O_5/TiO_2 catalysts prepared by a modified sol-gel method [5]. The results are discussed with respect of the distribution of vanadia as a function of V_2O_5 loading, in order to identify the vanadium species pairs and its coordination symmetry.

Experimental Section

Catalysts Preparation

V_2O_5/TiO_2 catalysts with different contents of V_2O_5 (wt% = 3, 6 and 9) were synthesized by a modified sol-gel method as previously described [5]. A sample containing only 1 wt% of V_2O_5 was made for the EPR analysis. Prior to acquisitions of Raman and EPR spectra, samples were first dried in vacuum at 503 K for 12 h. In the case of EPR, the samples were sealed in quartz tubes.

Raman Spectra

The Raman spectra were obtained using a 514.5 nm argon ion laser line (Spectra Physics) 2020, a Jobin-Yvon U1000 double monochromator with holographic gratings and a computer-controlled photon-counting system. The Raman spectra were obtained at room temperature as the average of 100 scans with a spectral resolution of 4 cm^{-1} using a power excitation of 45 mW.

EPR Spectra

The EPR experiments were carried out at both X and Q bands on powdered samples. All spectra were recorded as the first derivative of the absorption at 77 K. The Q band spectra were taken with an E-line Varian Spectrometer operating at 34 GHz, while for X band (9.6 GHz) the spectra were measured using a magnetic field modulation frequency of 85 KHz. Calibration of g-values was based on the $g = 1.9797$ signal of a $MgO:Cr^{3+}$ marker.

Results and Discussion

Raman Spectra

Raman spectra of the catalysts are presented in Fig. 1 and the vibrational modes are summarized in Table 1. The spectra show a well-defined absorption band at 1030 cm^{-1} and two broad bands from 900 to 960 cm^{-1} and 770 to 850 cm^{1}. The band at 1030 cm^{-1} is attributed to monomeric vanadyl species bound directly to the TiO_2 support [6, 12–16]. The number of bonds anchoring the vanadyl group to the support cannot be determined from the Raman spectra. These assignments are based on similarity of position of the bands in these regions with those for terminal V=O bonds of polyvanadate anions in solution. As the amount of polyvanadates increases, the number of terminal V=O groups per vanadium decreases to accommodate V—O—V linkages. The broad band in the region from 900 to 960 cm^{-1} and centered at 930 cm^{-1} is assigned to the terminal and internal V=O stretching

Table 1. Summary of Raman vibrational frequencies.

	Vibrational frequencies (cm^{-1})		
Loading %wt V_2O_5	Monomer ν(V=O)	ν(V—O—V)	Polymer ν(V=O)
3	1030	770–850	900–960
6	1030	770–850	900–960
9	1030	770–850	900–960

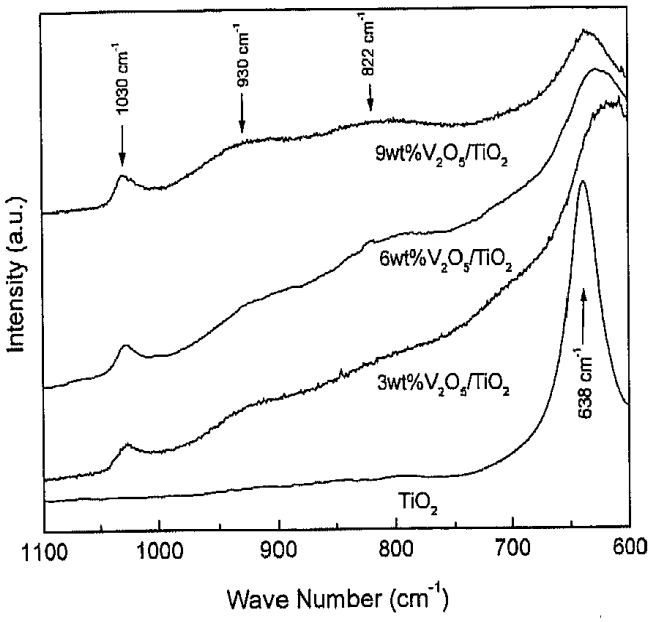

Figure 1. Raman Spectra of V_2O_5/TiO_2 samples obtained by a modified sol-gel method and dehydrated in vacuum at 503 K for 12 h.

vibration, ν(V=O), of polyvanadate groups and the broad band centered at 822 cm^{-1} can be attributed to the ν(V—O—V) vibration of polymeric vanadates [6, 12–16]. The Raman spectra do not exhibit bands at 997 and 703 cm^{-1}, characteristic of crystalline V_2O_5 [17], in agreement with those of X ray diffraction (XRD) [5] and are an indication of an effective distribution of vanadium in the titania matrix.

According to comparative FT-IR and Raman scattering studies, the vibrational frequencies of vanadate species do not depend strongly on the hydration/dehydration treatments [18]. The FT-IR spectra of the samples (Fig. 7 in [5]) present a sharp band around 1000 cm^{-1} and a broad band between 760 and 940 cm^{-1}. The intensities of these bands increases with increasing V_2O_5 content, but their width and their relative intensities remain unchanged. The Raman data agree well with the Infrared data. This indicates that the vanadyl/vanadate ratio is independent of vanadium concentration, and that the two species are uniformly distributed on the support.

EPR Spectra

The paramagnetic V^{4+} ion has the $3d^1$ electronic configuration and an electronic spin S = 1/2. The nuclear spin for the ^{51}V isotope (natural abundance 99.5%) is I = 7/2. Therefore, an eight component hyperfine structure is expected from the dipole-dipole interaction between the magnetic moment of the ^{51}V nucleus and the electronic moment of the paramagnetic V^{4+} ions. An axial spin Hamiltonian, which includes the hyperfine interaction has been used to describe the EPR spectra of V^{4+}:

$$H = g_{\parallel}\beta H_z S_z + g_{\perp}\beta(H_x S_x + H_y S_y) + A_{\parallel} I_z S_z + A_{\perp}(I_x S_x + I_y S_y) \quad (1)$$

where β is the Bohr magneton; H_x, H_y and H_z are the static magnetic field; S_x, S_y, and S_z are the spin operators of the electron; I_x, I_y, and I_z are the spin operators of the nucleus; $g_{\parallel}$ and $g_{\perp}$ are the parallel and perpendicular values of the anisotropic g-tensor; $A_{\parallel}$ and $A_{\perp}$ are the parallel and perpendicular hyperfine values of the hyperfine A-tensor.

One sample containing 1 wt% of V_2O_5 and calcined at 450°C was prepared for analyses of EPR in Q and X band. The relatively high quantity of vanadium in the samples (≥3 wt%) did not allow for the distinction of the signals due to hyperfine interaction.

The experimental V^{4+} EPR spectrum of the 1% V_2O_5/TiO_2 catalyst was analyzed by numerical simulation of the spin Hamiltonian (Eq. 1) using Lorentzian lineshapes. Fig. 2 shows the Q-band EPR absorption derivative spectra (experimental and simulated) of the 1%V_2O_5/TiO_2 catalyst measured at 77 K. The best fit of the experimental spectrum is achieved for the spin Hamiltonian parameters summarized in Table 2. The simulated spectrum closely reproduces the magnetic

Table 2. Spin-Hamiltonian parameters of the V^{4+} ions obtained by computer simulation of the spectrum (loading 1 wt%).

Signal	$g_{\parallel}$	$g_{\perp}$	$A_{\parallel}(G)$	$A_{\perp}(G)$	$\Delta H_{pp}(G)$
A	1.956	1.901	152.37	39.25	12.5
B	1.953	1.905–1.910	141.30	25–39	7.1
C		1.926			200

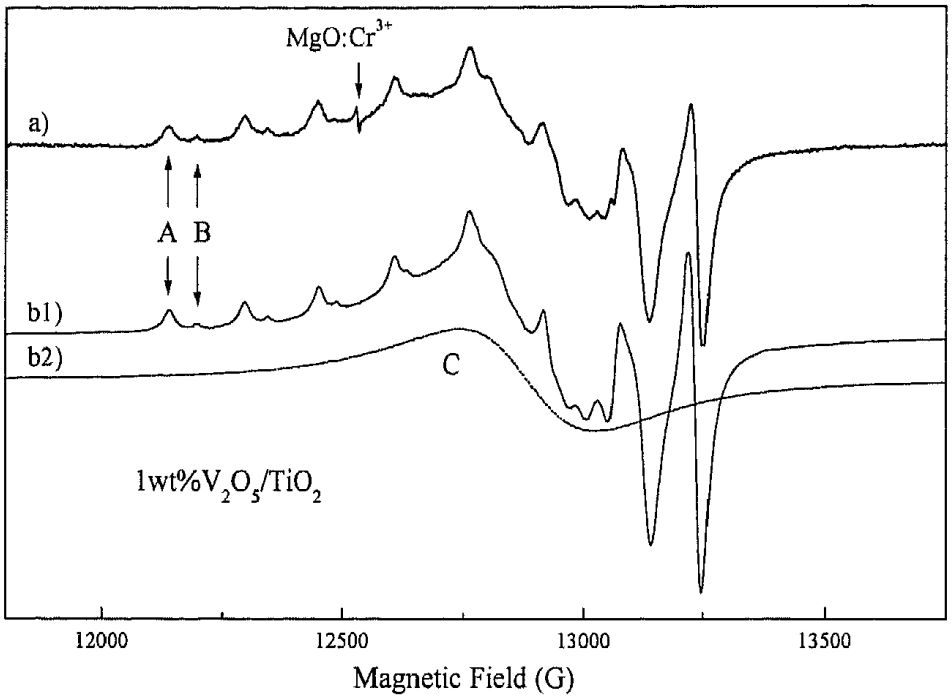

Figure 2. (a) Experimental and (b1) simulated EPR Q-band spectrum of 1 wt% V_2O_5 xerogel catalysts obtained at 77 K, (b1) hyperfine interactions and (b2) dipolar interaction. The MgO:Cr^{3+} ($g = 1.9797$) was used as reference signal.

field dependence of the experimental spectrum, the position and the intensities of the prominent features. The experimental spectrum is well resolved and can be interpreted as the superposition of the contribution of at least three families of V^{4+} ions: two sets of signals are characterized by an eight components structured EPR signals, species A and B in Fig. 2(a) and a third broad signal centered at $g \approx 1.93$ (hereafter referred as signal C).

The species A and B present a resolved hyperfine structure and are due to magnetically isolated V^{4+} ions. The broad and structureless signal C is due to magnetically interacting V^{4+} centers probably constituted by clusters or pairs of vanadium ions close enough to cause a dipolar broadening of the EPR line and the smearing the of ^{51}V hyperfine structure. Similar spectra were observed previously in V_2O_5/TiO_2 catalysts in both anatase and rutile form of TiO_2 [1, 3, 6–11].

The analysis of the EPR parameters of signals A and B show that species A differs from species B mainly in the value of the ^{51}V hyperfine constants ($A_\parallel$ and $A_\perp$), which are definitely higher for species A. The fact that $g_\parallel > g_\perp$ and $A_\parallel > A_\perp$ for both species suggests that the V^{4+} ions associated with these resonance are located at sites with octahedral symmetry, substituting for the Ti^{4+} ions in a titania matrix with the rutile structure [1, 10, 11, 13, 17, 19–25]. It should be remembered that the rutile phase of TiO_2 is tetragonal, with two Ti^{4+} ions per unit cell, and that each ion is surrounded by six neighboring oxygen atoms, giving rise to an orthorhombic crystal field at the titanium ion position. Therefore, in the rutile form of TiO_2 there are two nonequivalent Ti^{4+} ions whose positions can be occupied by substitutional V^{4+} ions [19]. Such a substitution is also favored as the ionic radius of Ti^{4+} and V^{4+} in a hexacoordinated octahedral crystal field are 0.74 Å and 0.72 Å, respectively [11]. A first alternative interpretation, where the isolated V^{4+} ions are located in interstitial sites of the rutile structure can be discarded since, in this case, an orthorhombic EPR spectrum is expected with $g_z < g_x < g_y$, which is not observed. A second alternative interpretation, in which V^{4+} ions are located in the anatase TiO_2 phase, is also discarded because, in this case, the g values for isolated ions should be $g_\parallel < g_\perp$ [2, 3, 13, 23–27].

As mentioned above, useful information about the environment of the vanadium ions can be obtained by the analysis of the spin Hamiltonian parameters. The empirical approach of Davidson and Che [11] uses a plot of $g_{iso} = (g_\parallel + 2g_\perp)/3$ and $A_{iso} = (A_\parallel + 2A_\perp)/3$ to describe the following ligand field geometries: (i) α, for vanadyl ions in a square-pyramidal or axially-distorted octahedral symmetry; (ii) β, for V^{4+} ions in a tetrahedral geometry and (iii) γ, for V^{4+} ions in a distorted octahedral symmetry. On the basis of the relatively low values found for both g_{iso} and A_{iso} in our samples

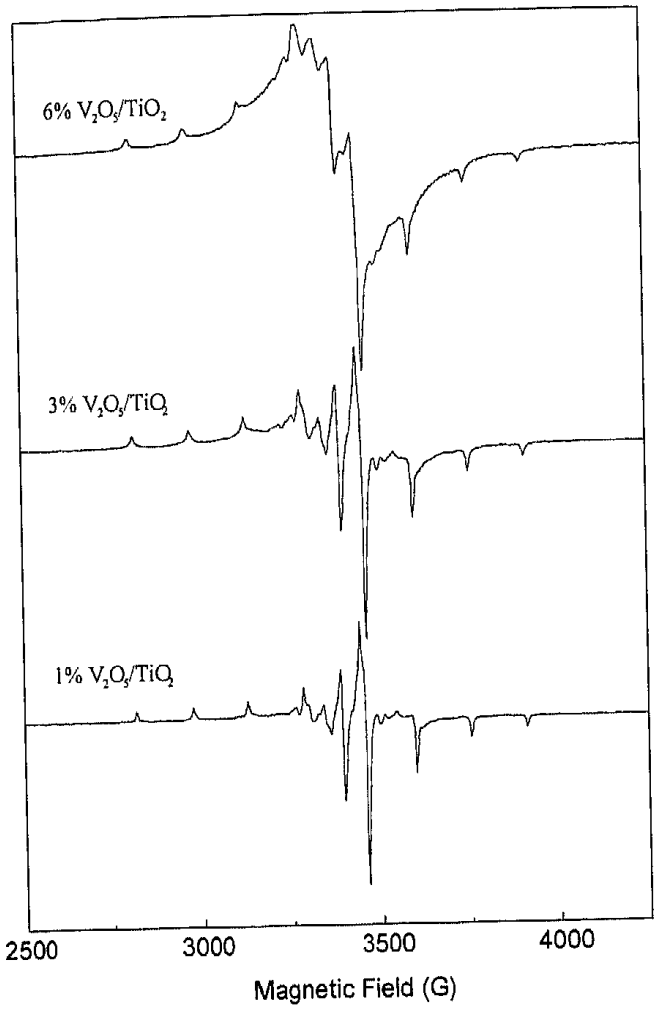

Figure 3. EPR X-band spectrum of 1, 3 and 6 wt% V_2O_5 samples.

($g_{iso} = 1.919$ and $A_{iso} = 77$ G for signal A, $g_{iso} = 1.92$ and $A_{iso} = 64$–73 G for signal B) we conclude that the magnetically isolated V^{4+} ions are subjected to a ligand field described by the geometry γ [Fig. 3 in Davidson and Che] where the vanadium ions are located at the center of the rutile unit cell, surrounded by a slightly distorted oxygen octahedron.

Figure 3 shows the X-band EPR spectra for samples with 1, 3 and 6 wt% V_2O_5. The spectrum of the catalysts with 3 wt% of V_2O_5 follows the general trends observed in Fig. 2. The EPR linewidths of the sample with the higher V_2O_5 concentrations (6 wt%) are significantly broader. This change on the EPR lineshape might be due to the interaction between V^{4+} ions resulting from the increase of the vanadia concentrations. The signals A and B associated with the parallel component of the isolated vanadium are observed in all samples, but in the X-band the distinction between these two signals is not as clear as in the Q-band spectra. The signal C corresponding to non-isolated vanadium ions is observed for all the V_2O_5 concentration investigated.

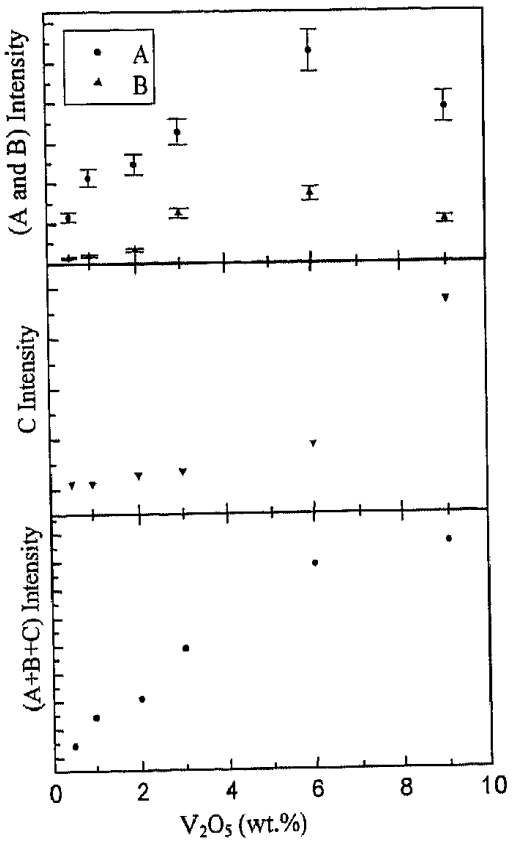

Figure 4. Evolution of the vanadium EPR intensity with V_2O_5 (wt%) content. The above graphic presents the V^{4+} isolated (A and B) signals. The interacting vanadium (C) signal is show in the middle graphic. The joint of the paramagnetic vanadium (A + B + C) is presented in the bottom graphic.

A detailed analysis allows us to extract the line width of the signal C, which is 200 G for the catalysts with lower loading ($\leq$6 wt%) and 250 G for the 9 wt% V_2O_5 catalysts.

Figure 4 presents the EPR intensity of signals A, B, C and total (A + B + C), obtained by doubly integrating the EPR signals, as a function of the V_2O_5 contents. The main results are summarized as follow. First, the signal A is always higher than the signal B. Second, the intensities of the signals A and B increase with the vanadia loading up to 6 wt% V_2O_5 and then decreases at higher vanadia content. In contrast, the intensity of the signal C increases very little with the vanadia content, up to 6 wt% V_2O_5, but an abrupt increase is observed for the higher concentration investigated (9 wt% V_2O_5). As the concentration of V_2O_5increases, the number of V^{4+} ions increases. This results in strong magnetic coupling among the V^{4+} ions, which are close enough to cause dipolar broadening. Third, the total V^{4+} signal intensity resulting from the sum of the signals A, B, and C species (Fig. 4, bottom) is proportional to the vanadia concentration up to 6 wt% V_2O_5.

Saturation of the total EPR signal is apparent above this concentration.

The results are in agreement with those of XRD and FT-IR measurement [5]. XRD has shown that the number of crystallites with rutile structure, which contribute to the A and B signals in the EPR spectra, decreases in relation to the anatase ones when increasing the vanadia concentration from 6 wt% to 9 wt% (Fig. 4 in [5]). This decrease of the amount of rutile phase is confirmed by EPR results of Fig. 4, which shows that the EPR intensities of signals A and B decrease at higher vanadia content. On the other hand, the FT-IR spectroscopy shows that the ratio between the amount of paramagnetic and diamagnetic vanadium ions, V^{4+}/V^{5+}, is nearly constant (Fig. 7 in [5]). Thus, the oxidation from V^{4+} to V^{5+} does not occur at the catalyst surface. As the EPR intensities of signals A and B decrease at higher vanadia content, whereas the intensity of signal C increases significantly, it is concluded that a partial oxidation of V^{4+}/V^{5+} takes place at higher concentration of V_2O_5, leading to the observed saturation of the total EPR signal (Fig. 4, bottom). The oxidation of the V^{4+} in TiO_2 rutile was already observed by Centi et al. [7].

Conclusions

Raman Spectroscopy was used to investigate the distribution of VO_x species on the surface of TiO_2 in the catalysts prepared by a modified sol-gel method. Two species of surface vanadium have been identified: monomeric vanadyl and polymeric vanadates. Monomeric vanadyls are characterized by a narrow Raman band at 1030 cm^{-1} and polymeric vanadates by two broad bands between 900 and 960 cm^{-1} and 770 to 850 cm^{-1}. Raman spectra of samples do not exhibit a characteristic peak of crystalline V_2O_5. These results are in agreement with those of XRD and FT-IR measurements [5]. They indicate uniform distribution of vanadium in the titania matrix.

EPR technique was used to obtain information about the nature of the vanadium species and their distribution in V_2O_5/TiO_2 catalysts. At least three families of V^{4+} ions were identified. The analysis of the EPR spectra suggests that isolated V^{4+} ions are located in sites with octahedral symmetry substituting Ti^{4+} ions in the rutile structure. Magnetically interacting V^{4+} ions are also present as pairs or clusters giving rise to a broad and structureless EPR line. At higher concentration of V_2O_5, a partial oxidation of V^{4+} (paramagnetic) to V^{5+} (diamagnetic) is apparent from the EPR results.

Acknowledgment

The authors are grateful to the FAPESP, CNPq and FUNDUNESP Foundations (Brazil) for financial support and to Dr. O.R. Nascimento and A.J. Da Costa Filho for their help in the Q-band EPR measurements.

References

1. F. Cavani, G. Centi, E. Foresti, F. Trifirò, and G.J. Busca, Chem. Soc. Faraday Trans. **84**, 237 (1988).
2. K.V.R. Chary, G. Kishan, T. Bhaskar, and C.J. Sivaraj, Phys. Chem. B **102**, 6792 (1998).
3. L. Dall'Acqua, M. Baricco, F. Berti, L. Lietti, and E.J. Giamello, Mater. Chem. **8**, 1441 (1998).
4. G.C. Bond, Appl. Catal. A **157**, 91 (1997).
5. C.B. Rodella, R.W.A. Franco, C.J. Magon, J.P. Donoso, L.A.O. Nunes, M.J. Saeki, M.A. Aegerter, V. Sargentelli, and A.O. Florentino, J. Sol-Gel Science and Technology, submitted.
6. G.T. Went, L.-J. Leu, R. Rosin, and A.T. Bell, J. Catal. **134**, 492 (1992).
7. G. Centi, E. Giamello, D. Pinelli, and F.J. Trifirò, J. Catal. **130**, 220 (1991).
8. M.C. Paganini, L. Dall'Acqua, E. Giamello, L. Lietti, P. Forzatti, and G. Busca, J. Catal. **166**, 195 (1997).
9. L.J. Alemany, L. Lietti, N. Ferlazzo, P. Forzatti, G. Busca, E. Giamello, and F. Bregan, J. Catal. **155**, 117 (1995).
10. A. Aboukaïs, C.F. Aissi, M. Dourdin, D. Courcot, M. Guelton, E.M. Serwicka, E. Giamello, F. Geobaldo, A. Zecchina, A. Foucault, and J.C. Vedrine, Catal. Today **20**, 87 (1994).
11. A. Davidson and M. Che, J. Phys. Chem. **96**, 9909 (1992).
12. G.T. Went, L.-J. Leu, and A.T. Bell, J. Catal. **134**, 479 (1992).
13. V. Luca, S. Thomson, and R.F. Howe, J. Chem. Soc., Faraday Trans. **93**, 2195 (1997).
14. G. Busca, L. Marchetti, G. Centi, and F. Trifirò, Langmuir **2**, 568 (1986).
15. F. Prinetto, G. Ghiotti, M. Occhiuzzi, and V. Indovina, J. Phys. Chem. B **102**, 10316 (1998).
16. C.C.P. Forzatti and G. Busca, J. Catal. **116**, 586 (1989).
17. S.S. Chan, I.E. Wachs, L.L. Murrell, L. Wang, and W. Keith Hall, J. Phys. Chem. **88**, 5381 (1984).
18. A. Vejux and P. Courtine, J. Solid State Chem. **23**, 93 (1978).
19. G.M. Zverev and A.M. Prokhorov, JETP **39**, 222 (1960).
20. H.J. Gerritsen and H.R. Lewis, Phys. Rev. **119**, 1010 (1960).
21. R.S. Biasi and A.A.R. Fernandes, J. Am. Ceram. Soc. **79**, 2179 (1996).
22. F. Kubec and Z. Sroubek, J. Chem. Phys. **57**, 1660 (1972).
23. M. Grätzel and R.F. Howe, J. Phys. Chem. **94**, 2566 (1990).
24. R. Gallay, J.J. Van der Klink, and J. Moser, Phys. Rev. **34**, 3060 (1986).
25. V. Luca, D.J. MacLachlan, and R. Bramley, JCCP **1**, 2597 (1999).
26. A.A. Altynnikov, G.A. Zenkovets, and V.F. Anufrienko, React. Kinet. Catal. Lett. **66**(1), 85 (1999).
27. K.V. Narayana, A. Venugopal, K.S. Rama Rao, S. Khaja Masthan, V. Venkat Rao, and P. Kanta Rao, Appl. Catal. A. **167**, 11 (1998).